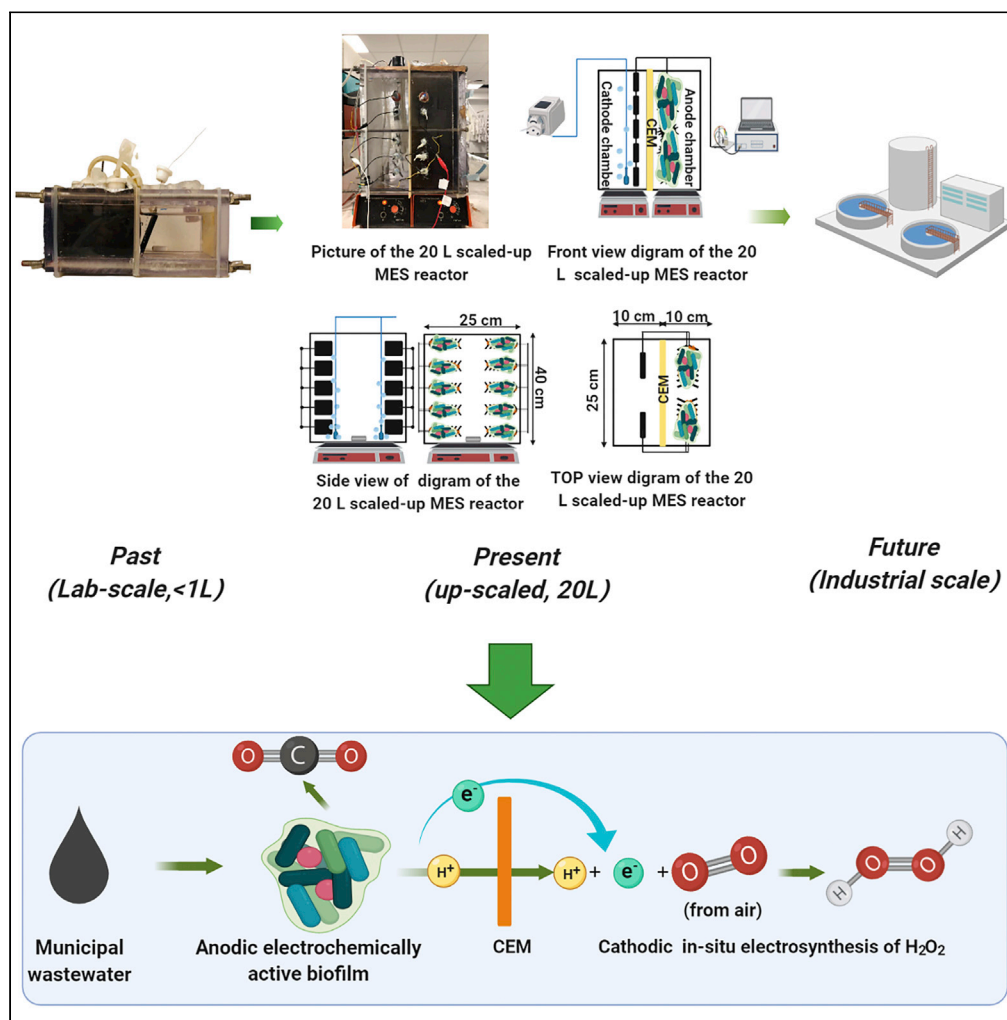**Article**

Scaling-up of microbial electrosynthesis with multiple electrodes for *in situ* production of hydrogen peroxide

Rusen Zou, Aliyeh Hasanzadeh, Alireza Khataee, Xiaoyong Yang, Mingyi Xu, Irini Angelidaki, Yifeng Zhang

yifz@env.dtu.dk,
yifzmfc@gmail.com

HIGHLIGHTS

Up-scaled microbial electrosynthesis with multiple electrodes to synthesize H_2O_2

The H_2O_2 yield was higher than that of laboratory-scale systems using graphite cathode

Energy consumption was lower than that of laboratory-scale (bio) electrochemical systems

Systematic evaluation of the influence of operating parameters on H_2O_2 production

Article

Scaling-up of microbial electrosynthesis with multiple electrodes for *in situ* production of hydrogen peroxide

Rusen Zou,[1] Aliyeh Hasanzadeh,[2] Alireza Khataee,[3,4] Xiaoyong Yang,[1] Mingyi Xu,[1] Irini Angelidaki,[1] and Yifeng Zhang[1,5,*]
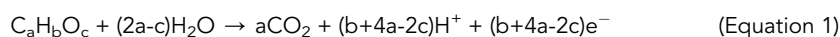
SUMMARY

Microbial electrosynthesis system (MES) has recently been shown to be a promising alternative way for realizing *in situ* and energy-saving synthesis of hydrogen peroxide (H_2O_2). Although promising, the scaling-up feasibility of such a process is rarely reported. In this study, a 20-L up-scaled two-chamber MES reactor was developed and investigated for *in situ* and efficient H_2O_2 electrosynthesis. Maximum H_2O_2 production rate of 10.82 mg L^{-1} h^{-1} and cumulative H_2O_2 concentration of 454.44 mg L^{-1} within 42 h were obtained with an input voltage of 0.6 V, cathodic aeration velocity of 0.045 mL min^{-1} mL^{-1}, 50 mM Na_2SO_4, and initial pH 3. The electrical energy consumption regarding direct input voltage was only 0.239 kWh kg^{-1} H_2O_2, which was further much lower compared with laboratory-scale systems. The obtained results suggested that the future industrialization of MES technology for *in situ* synthesis of H_2O_2 and further application in environmental remediation have broad prospects.

INTRODUCTION

Hydrogen peroxide (H_2O_2) is a green and environment-friendly oxidant that has been widely used in industrial and environmental applications (Kelly et al., 2019; Sheng et al., 2020; Zhao et al., 2020). According to statistics, the world's H_2O_2 production capacity exceeded 5 million tons in 2015 and maintained steady growth, most of which were synthesized based on the anthraquinone method, which has the disadvantage of high energy consumption and high-risk coefficient (Sheng et al., 2020; Zhao et al., 2020). In addition, due to the unstable chemical properties of H_2O_2, this also provides challenges for transportation and storage and correspondingly increases costs (Chen et al., 2018). For many applications, such as advanced oxidation processes for water treatment, the required concentration of H_2O_2 was usually below 1,000 mg L^{-1}. In this context, it is urgent and important to develop alternative methods for the *in situ* synthesis of H_2O_2. In the past years, among others, electrochemical methods have received extensive attention due to their relatively high H_2O_2 synthesis efficiency and easy operation (only need electrical energy as input) (Campos-Martin et al., 2006; Siahrostami et al., 2013). Despite its promise, the electrochemical methods are still suffering from the disadvantage of large energy costs (Perry et al., 2019).

Recently, the microbial electrosynthesis system (MES), in which electrochemically active microorganisms can obtain energy from the oxidation of organics in sewage, have been demonstrated as an efficient and cost-effective means for the production of H_2O_2 (Hassan et al., 2019; Li et al., 2018a, 2018b·bib_Li_et_al_2018a; Zhao et al., 2020). Specifically, in a typical two-chamber MES, the anodic electrochemically active microorganisms can oxidize organic matter in wastewater and generate electrons, protons, and carbon dioxide via Equation (1) (Hassan et al., 2019). Among them, the generated electrons and protons are further transferred to the cathode chamber through wires and cation exchange membrane (CEM), respectively, and are further combined with oxygen to generate H_2O_2 through two-electron reduction via Equation (2) (Hassan et al., 2019).

$$C_aH_bO_c + (2a-c)H_2O \rightarrow aCO_2 + (b+4a-2c)H^+ + (b+4a-2c)e^- \quad \text{(Equation 1)}$$

$$O_2 + 2H^+ + 2e^- \rightarrow H_2O_2 \quad \text{(Equation 2)}$$

[1]Department of Environmental Engineering, Technical University of Denmark, 2800 Lyngby, Denmark

[2]Process and Systems Engineering Center (PROSYS), Department of Chemical and Biochemical Engineering, Technical University of Denmark, Kgs. Lyngby, Denmark

[3]Research Laboratory of Advanced Water and Wastewater Treatment Processes, Department of Applied Chemistry, Faculty of Chemistry, University of Tabriz, 51666-16471, Tabriz, Iran

[4]Peoples' Friendship University of Russia (RUDN University), 6 Miklukho-Maklaya Street, Moscow, 117198, Russian Federation

[5]Lead contact

*Correspondence: yifz@env.dtu.dk, yifzmfc@gmail.com

https://doi.org/10.1016/j.isci.2021.102094

To this end, the microbial fuel cell (MFC) and its derived microbial electrolysis cell (MEC)-based MES have been proposed for H_2O_2 production, and the range of produced H_2O_2 was 79–1,300 mg L^{-1} (Li et al., 2017). This production level would be able to satisfy the application in the water treatment process. Nonetheless, it was worth noting that most of the MES studies on the *in situ* synthesis of H_2O_2 including MFC or MEC were conducted with laboratory-scale reactors ranging from milliliters to hundreds of milliliters. Scaling-up is of importance to prove the feasibility and economic profits of such a process for large-scale application. However, a systematic evaluation of the scaling-up of MES for H_2O_2 synthesis is rarely reported. So far, the only scaling-up study was reported by Sim et al. who developed a 110-L dual-chamber up-scaled MEC reactor (10 L of cathode chamber and 1.6–2.0 V voltage input) to synthesize H_2O_2. Nevertheless, the H_2O_2 titer was less than 100 mg L^{-1} after 20 days of operation, and the corresponding H_2O_2 conversion efficiency was only about 7.2% in a form of short communication (Sim et al., 2018). Thus, more efforts are required toward the scaling-up of the MES-based H_2O_2 production. Among others, the electrode material is one of the important factors for a successful scaling-up, which is directly related to the current efficiency (CE), two-electron oxygen reduction reaction (ORR) selectivity (Equation (2)), and energy consumption during the *in situ* electrosynthesis of H_2O_2 in the cathode. In traditional MFC for bioelectricity production, noble metals (e.g., titanium and platinum) are usually used as electrode materials or catalysts for favoring four-electron oxygen reduction to produce H_2O via Equation (3) (Chung et al., 2020; Hassan et al., 2019).

$$O_2 + 4H^+ + 4e^- \rightarrow 2H_2O \qquad \text{(Equation 3)}$$

In contrast, carbon-based electrodes without containing noble metals, especially the commonly used graphite-based electrodes such as graphite plate and graphite felt, are often applied in the electrosynthesis of H_2O_2 given their merits of strong electrical conductivity, high two-electron ORR selectivity, inexpensive, long lifetime, weak H_2O_2 decomposition effect, and ease of scaling up (An et al., 2019; Chung et al., 2020; Li et al., 2016, 2017). In addition, it should be noted that although most of the current laboratory-scale studies related to bioelectrochemical synthesis of H_2O_2 used gas diffusion electrodes (GDE) as the cathode to obtain a high H_2O_2 yield, their mechanical property makes it difficult to be scaled up (Li et al., 2016). Moreover, the effect of acidic pH (2–3) on the stability of the GDE and the formation of possible refractory by-products are two main challenges for *in situ* wastewater treatment (Wang et al., 2020a). In addition, almost all these laboratory-scale MES reactors were only equipped with a single electrode including a bio-anode and an abiotic cathode in each chamber, which tended to cause system instability.

This study successfully scaled up an MES with multiple graphite electrodes to 20 L (dual-chamber and 10 L of each chamber) and comprehensively investigated the influence of operating parameters including input voltage, cathodic aeration velocity, catholyte pH, and electrolyte nature and concentration on the *in situ* synthesis of H_2O_2. To the best of our knowledge, this is the first scaled-up MES reactor equipped with highly stable graphite plate electrodes for *in situ* H_2O_2 synthesis. The present study not only verified the feasibility of such scaled-up MES for H_2O_2 synthesis but also accumulated valuable experience for subsequent industrial applications on the treatment of wastewater.

RESULTS AND DISCUSSION

The performance of 20-L scaled-up MES reactor for H_2O_2 synthesis

A series of experiments was carried out to demonstrate the feasibility of the 20-L scaled-up MES reactor for H_2O_2 synthesis. Figure 1 shows the change of H_2O_2 concentration with operating time at the cathode in the 20-L scaled-up MES reactor. The concentration of H_2O_2 increased monotonically with operating time and reached about 454.44 mg L^{-1} at 42 h. Specifically, the synthesis rate of H_2O_2 in the first 16 h was significantly higher than that in the next 26 h; especially after 36 h, the increase of H_2O_2 concentration was relatively slow. Moreover, the cathodic pH varied during the process (Figure S1). A rapid rise in pH was observed as the reaction progressed. The cathodic pH reached 8.58 in the first 16 h, and then gradually increased and finally reached 10.07 at 42 h. The fast increase of pH observed in the first 16 h was due to the fast reduction of two electrons of oxygen to H_2O_2 via Equation (2). After that, when the cathodic pH turned to alkaline, the main reaction occurring on the cathode surface was the reduction of oxygen to HO_2^- via Equation (4) (Brillas et al., 1997; Moreira et al., 2017).

$$O_2 + H_2O + 2e^- \rightarrow HO_2^- + OH^- \qquad \text{(Equation 4)}$$

In addition, the *in situ*-generated H_2O_2 would be further reduced to H_2O and OH^- under acidic or alkaline conditions via Equations (5) and (6), respectively, and the decomposition of H_2O_2 would also occur
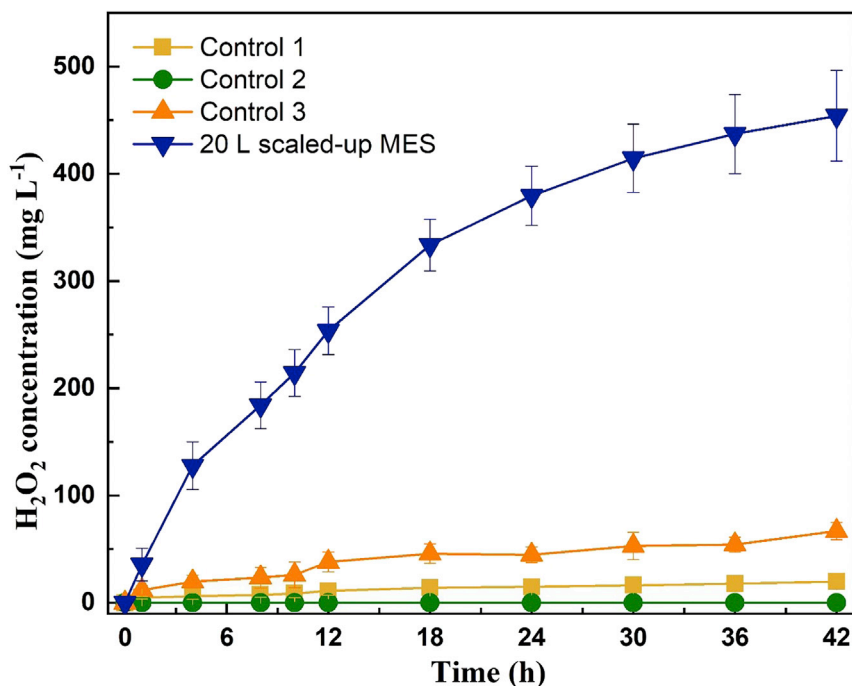
Figure 1. Feasibility verification of this 20-L scaled-up MES reactor regarding H₂O₂ production

Operating conditions: input voltage of 0.6 V, cathode aeration velocity of 0.045 mL min^{-1} mL^{-1}, initial catholyte pH of 3, and electrolyte nature and concentration of 50 mM Na$_2$SO$_4$, respectively. Control 1: without cathodic aeration. Control 2: open circuit. Control 3: without input voltage.

simultaneously via Equations (7) and (8), thus more H$_2$O$_2$ would be decomposed in a longer operating time (Nidheesh and Gandhimathi, 2012; Qiang et al., 2002; Xia et al., 2015). In short, the above-mentioned results also proved the feasibility of the graphite plate as the cathode of this scaled-up reactor for two-electron ORR to generate H$_2$O$_2$ via Equation (2).

$$H_2O_2 + 2H^+ + 2e^- \rightarrow 2H_2O \qquad \text{(Equation 5)}$$

$$HO_2^- + H_2O + 2e^- \rightarrow 3OH^- \qquad \text{(Equation 6)}$$

$$2H_2O_2 \rightarrow O_2 + 2H_2O \qquad \text{(Equation 7)}$$

$$H_2O_2 + OH^- \rightarrow HO_2^- + H_2O \qquad \text{(Equation 8)}$$

Besides, the control experiments including the MES reactor without cathodic aeration (control 1), open circuit (control 2), and without input voltage (control 3) were also conducted and the results were also exhibited in Figure 1. As expected, no H$_2$O$_2$ production was detected when the system was in an open circuit. According to Equation (2), as no electrons were flowing from the anode to the cathode in the open-circuit state, there was no H$_2$O$_2$ produced. Similarly, the reactor without cathodic aeration or input voltage (corresponding to operating at MFC mode) only produced a low concentration of H$_2$O$_2$ (below 20 and 70 mg L^{-1}, respectively). The low H$_2$O$_2$ production could be attributed to insufficient oxygen or electrons for the synthesis of H$_2$O$_2$ based on Equation (2). Similar results were also found in the previous studies by using a laboratory-scale MES and electrochemical system (Li et al., 2017; Yu et al., 2015a). Therefore, the obtained results highlighted that the reactor operating in MEC mode (requiring a small amount of voltage input) was effective and superior in H$_2$O$_2$ productivity compared with operating in MFC mode. However, it is worth emphasizing that around 70 mg L^{-1} of H$_2$O$_2$ was still produced when this scaled-up reactor was operated in the MFC mode, which further proved that the scaled-up reactor can generate enough H$_2$O$_2$ to meet the

water and wastewater treatment requirements (e.g., 5–50 mg L^{-1} of H_2O_2 were needed for water disinfection and micro-pollutant removal) (Chung et al., 2020).

In addition to studying the H_2O_2 synthesis at the cathode, we also monitored the current and cathode potential of the system under different conditions. As depicted in Figure S1, the stable and relatively high current density output (around 2.86 A m^{-2}) together with a stable cathode potential (around −0.6 V) were observed during the entire operation, respectively. It proved that the biological anode of this scaled-up system was stable during the test. Furthermore, as the performance of the *in situ* synthesis of H_2O_2 via MES has been shown to depend on the transfer of effective microbial electrons to the anode (Logan and Regan, 2006), the observed stable current output demonstrated the feasibility of further application of large-scale MES *in situ* synthesis of H_2O_2 in the future. In contrast, the current density outputs obtained in the control conditions (around 1.25, 0, and 0.56 A m^{-2}) were significantly lower than the normal operating condition.

Overall, the above-mentioned results proved that the scaled-up MES reactor with sufficient cathodic aeration and electron flow can provide stable and efficient *in situ* production of H_2O_2.

Effect of operating parameters

Input voltage

The H_2O_2 synthesis was generally slow in MFC mode due to the low circuit current (Li et al., 2017). As an alternative, H_2O_2 production can be significantly increased by applying a small amount of applied voltage (normally below 0.8 V) in MEC mode. In general, a higher input voltage would lead to a higher current, thus the enhanced electron flow would increase the rate of H_2O_2 synthesis. However, it would not be the case, because the higher input could also promote the occurrence of side reactions, resulting in a decrease in current efficiency, and produce similar or even lower H_2O_2 yields compared with lower input voltage (Moreira et al., 2017; Oturan et al., 2018). Therefore, seven groups of different input voltages (0.1, 0.2, 0.4, 0.5, 0.6, 0.7, and 0.8 V) were selected to investigate their influence on H_2O_2 synthesis. As shown in Figure 2A, the cumulative H_2O_2 production in 42 h was 125.36, 236.36, 314.93, 353.40, 454.44, 408.70, and 385.71 mg L^{-1}, respectively, at the input voltage ranging from 0.1 to 0.8 V. The results indicated that the optimum input voltage was 0.6 V and further increasing the input voltage (0.7 and 0.8 V) led to a decrease in H_2O_2 production. Likewise, the variation trend of current efficiency presented in Figure 2B was also in line with the yield of H_2O_2, and the corresponding values were 1.63%, 2.42%, 2.80%, 3.41%, 2.66%, and 2.37% at input voltage ranging from 0.1 to 0.8 V, respectively. The system current and cathode potential were shown in Figure S2, respectively. It was observed that both system current density (from 1.63 to 3.44 A m^{-2}) and cathode potential (in terms of absolute value, from −0.45 to −0.66 V) increased continuously with the increase of the applied voltage from 0.1 to 0.8 V. Thus, the aforementioned results can be explained from two aspects. On the one hand, the increase of current density led to accelerated electron transfer on the surface of the cathode electrode, thereby promoting oxygen reduced to the H_2O_2 via Equation (1) (Yu et al., 2015a, 2015b). On the other hand, higher currents may also enhance the occurrence of side reactions, such as accelerating the conversion of the produced H_2O_2 into H_2O via Equations (5), (7), and (8); even reduction of oxygen to H_2O via Equation (3) (Chen et al., 2015a; Nadais et al., 2018; Wang et al., 2020b); or hydrogen evolution via Equation (9) (Chen et al., 2015a).

$$2H^+ + 2e^- \rightarrow H_2 \qquad \qquad \text{(Equation 9)}$$

Similar results were also observed in the previous studies regarding abiotic electro or MES for H_2O_2 production (Chen et al., 2015a; Li et al., 2016; Yu et al., 2015a). Notably, the highest H_2O_2 yield (at 0.6 V) obtained in this study was around 10.82 mg L^{-1} h^{-1}, which was about 3.3 times higher than that observed in the highest value from laboratory-scale (cathodic working volume of 14 mL) MEC reactor (3.92 mg L^{-1} h^{-1}) (Li et al., 2016). Moreover, it was also found that the production rate of H_2O_2 was slightly higher than that of the laboratory-scale (cathodic working volume of 100 mL) MES reactor is driven by salinity gradient (10.80 mg L^{-1} h^{-1}) (Li et al., 2017). Taking into account the H_2O_2 production rate, the current efficiency, and the energy consumption, an input voltage of 0.6 V was the optimal value among the investigated voltages.

Cathodic aeration rate

As observed in the previous part, the cathode aeration was essential to H_2O_2 production. However, it was not that the faster the aeration rate, the higher the concentration of H_2O_2 produced at the cathode. Excess aeration could reduce H_2O_2 production and also increase energy consumption. Thus, set an optimal aeration rate could
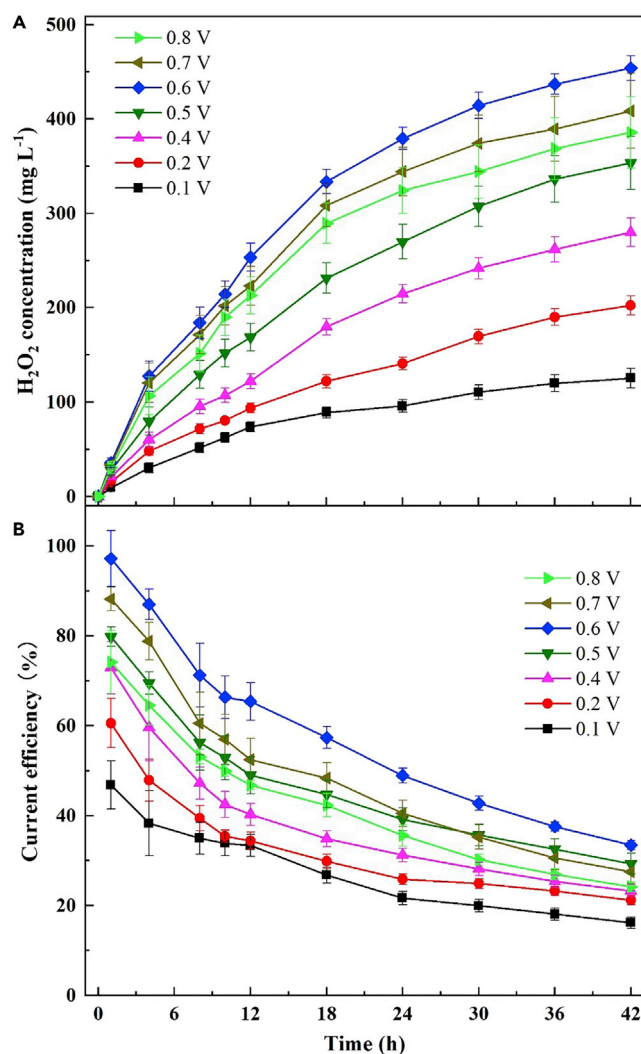
Figure 2. Effect of input voltage

(A) H_2O_2 production and (B) current efficiency in the scaled-up reactor. Operating conditions: cathode aeration velocity of 0.045 mL min^{-1} mL^{-1}, initial catholyte pH of 3, and electrolyte nature and concentration of 50 mM Na_2SO_4, respectively.

not only maximize the H_2O_2 production at the cathode but could also save energy consumption. In this part, the aeration rates ranging from 4 to 500 mL min^{-1}, corresponding to the cathode aeration velocities of 0.00045–0.056 mL min^{-1} mL^{-1}, were adopted to study its effect on the H_2O_2 synthesis at the cathode. As shown in Figure 3, the H_2O_2 concentration accumulated at the cathode increased monotonically with the increase of the aeration rate in 42 h, which indicated that the selected aeration rate range has no negative effect on the H_2O_2 production at the cathode. When the aeration velocity was increased from 0.045 to 0.056 mL min^{-1} mL^{-1}, the accumulated H_2O_2 concentration only increased slightly (from 454.44 to 459.30 mg L^{-1}). Additionally, the concentration of cathodic DO also increased with the increase of aeration velocity (Figure 3). Among them, it can be seen that when the aeration velocity was lower than 0.045 mL min^{-1} mL^{-1}, the catholyte was unsaturated, whereas the catholyte was in a saturated or supersaturated state when the aeration rate reached 0.045 mL min^{-1} mL^{-1} or above. These results were in agreement with previous studies using photocatalytic or photo-assisted electrocatalytic processes for H_2O_2 production (Salmerón et al., 2019; Yu et al., 2018). The increased aeration rate increased the catholyte DO and promoted the mass transfer rate of oxygen in the catholyte, which was beneficial to the production of H_2O_2 (Luo et al., 2015a; Yu et al., 2015a). When the aeration rate was increased from 400 to 500 mL min^{-1}, the insignificant increase in the accumulated H_2O_2 concentration could be due to the following reasons. First, the increase in the number of bubbles generated by aeration would
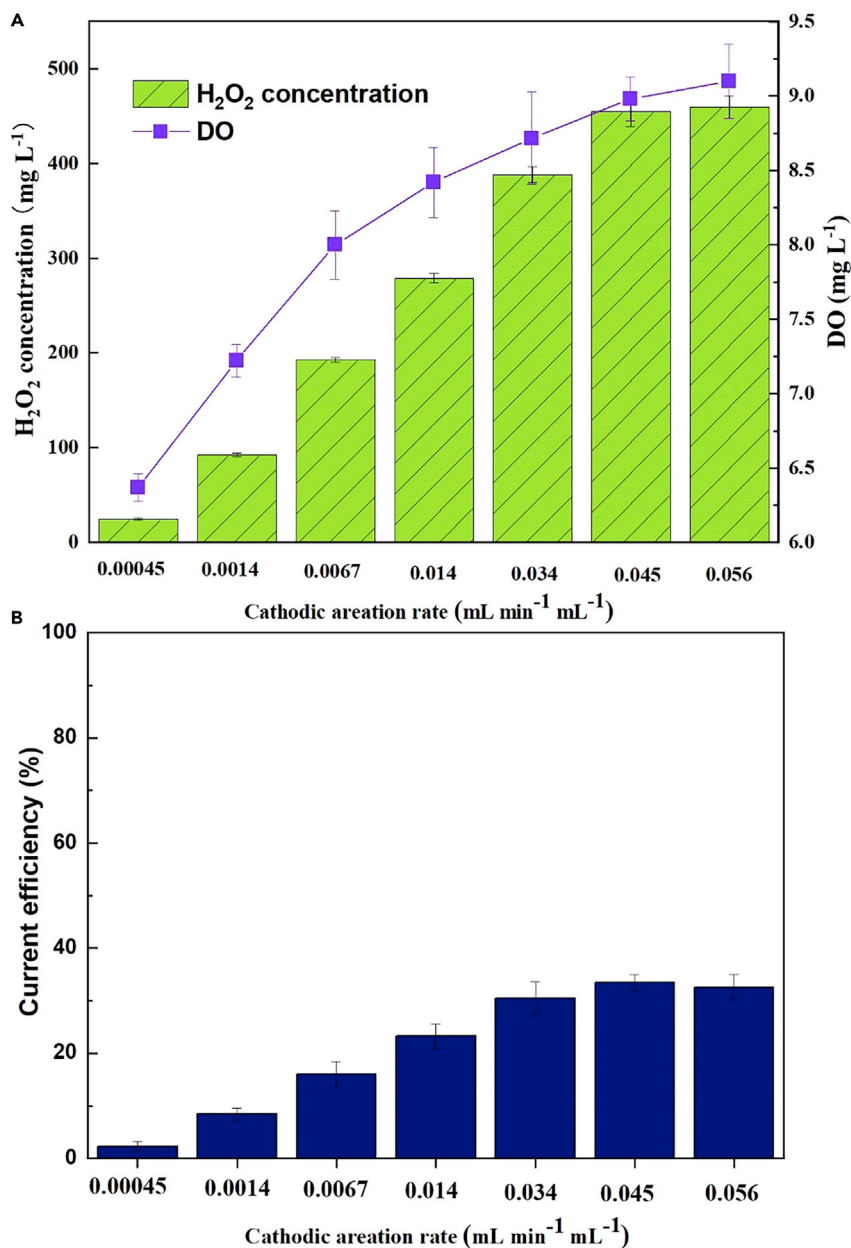
impact of initial catholyte pH (3, 5, 7, and 9) on the cathodic electrosynthesis of H_2O_2 was studied. The results showed that the change of initial pH significantly affected the cathodic synthesis of H_2O_2, and cumulative concentration reached approximately 454.44, 412.71, 395.71, and 316.36 mg L^{-1}, respectively, after 42-h operation (Figure 4A). Similarly, the current efficiency and H_2O_2 rates also showed the same variation trend, resulting in final values of 3.41%, 3.10%, 2.97%, and 2.37% and 10.82, 9.83, 9.42, and 7.53 mg L^{-1} h^{-1}, respectively (Figures 4B and S4). In addition, the change of catholyte pH value over time was shown in Figure 4C. The rapid rise of pH indicated that the consumption rate of protons at the cathode for the synthesis of H_2O_2 was faster than the generation rate at the anode (latterly entered the cathode through the CEM). As mentioned previously, under alkaline conditions, especially at pH > 9, H_2O_2 mainly existed in the form of HO_2^-, which could catalyze the decomposition of H_2O_2 via Equation (10) (Luo et al., 2015b; Sheng et al., 2011).

$$H_2O_2 + HO_2^- \rightarrow {}^{\cdot}OH + {}^{\cdot}O_2^- + H_2O \qquad \text{(Equation 10)}$$
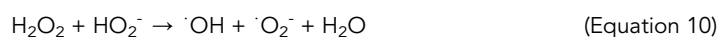
This also explained why the cumulative H_2O_2 concentration was lower with the initial pH 9 than with other pH values. The same experimental results were found in the electrochemical synthesis of H_2O_2 using unmodified graphite electrodes (Yu et al., 2015a). Therefore, when the initial pH was set to 3, more H_2O_2 can be synthesized at the cathode, and this value conformed to the optimal pH range (2–4) of the traditional electro-Fenton and bio-electro-Fenton processes (Li et al., 2018a, 2018b; Moreira et al., 2017). It should be noted that the cumulative H_2O_2 concentration under the neutral and alkaline conditions observed in this study still meet the needs of water treatment, which may broaden the applicability of the scaled-up MES in other fields such as combining other technologies (e.g., UV-based advanced oxidation processes) or catalysts for water treatment. In this way, it may also reduce the chemical cost, as there was no need to use acid and alkali to adjust the pH before water treatment.

Electrolyte nature and concentration

Generally, research processes related to electrochemical systems required high conductivity in the electrolyte to enhance the flow of electrons. In this study, we have selected three widely used electrolytes including Na_2SO_4, NaCl, and Na_2CO_3 with an initial concentration of 50 mM to explore their effects on the synthesis of H_2O_2 at the cathode. As presented in Figures 5A and 5B, when Na_2SO_4 was used as the electrolyte, the accumulated H_2O_2 concentration in 42 h was 454.44 mg L^{-1}, followed by Na_2CO_3 and NaCl (358.50 and 262.17 mg L^{-1}, respectively). The reasons why Na_2SO_4 as an electrolyte was superior to Na_2CO_3 and NaCl can be explained as follows: (1) chloride ion in NaCl could react with H_2O_2 to generate higher reactive HClO and/or chlorine derivatives via Equation 11–18 (De Laat et al., 2004; Lai et al., 2020; Moreira et al., 2017); (2) CO_3^{2-} itself and its hydrolysis product HCO_3^- (main role) could cause the decomposition of H_2O_2 via Equation 19–22 (Attiogbe and Francis, 2011; Fabian, 1995; Xia et al., 2020);

$$H_2O_2 + Cl^- \rightarrow ClO^- + H_2O \qquad \text{(Equation 11)}$$

$$H_2O_2 + ClO^- \rightarrow Cl^- + O_2 + H_2O \qquad \text{(Equation 12)}$$

$$H_2O_2 + e^- \rightarrow {}^{\cdot}OH + OH^- \qquad \text{(Equation 13)}$$

$${}^{\cdot}OH + Cl^- \rightarrow {}^{\cdot}ClOH^- \qquad \text{(Equation 14)}$$

$${}^{\cdot}ClOH^- + Cl^- \rightarrow {}^{\cdot}Cl_2^- + OH^- \qquad \text{(Equation 15)}$$

$${}^{\cdot}Cl_2^- \rightarrow {}^{\cdot}Cl + Cl^- \qquad \text{(Equation 16)}$$

$${}^{\cdot}Cl_2^- + H_2O_2 \rightarrow {}^{\cdot}HO_2 + H^+ + 2Cl^- \qquad \text{(Equation 17)}$$

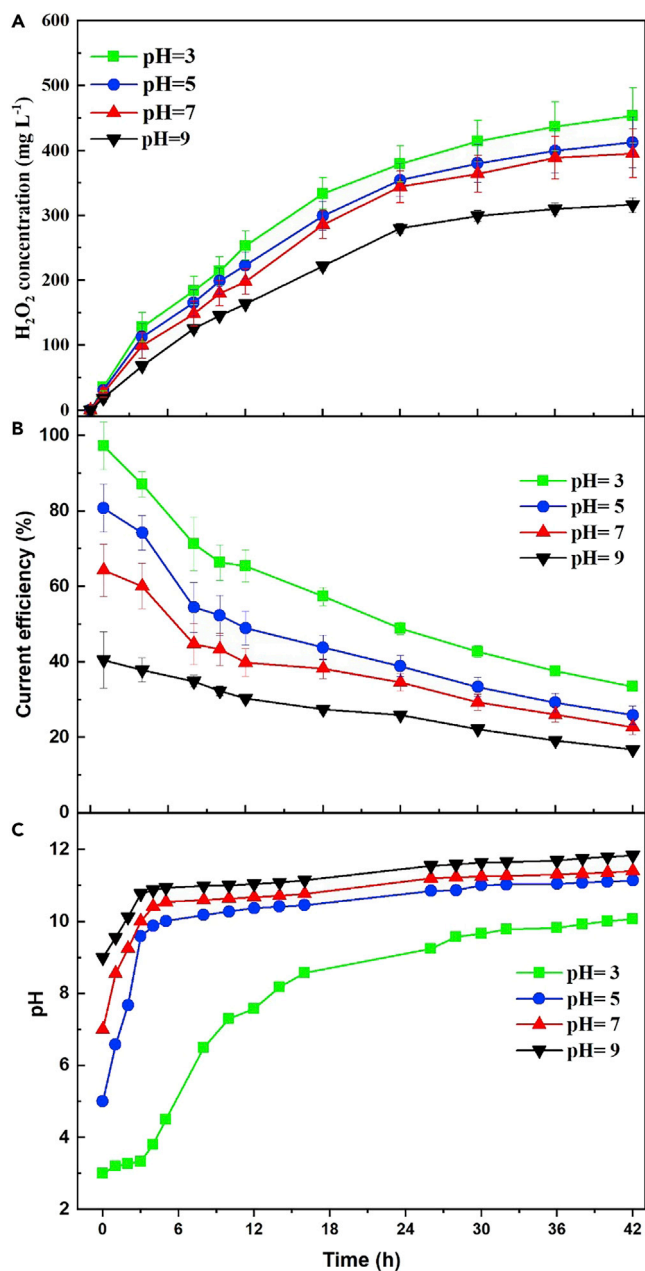$${}^{\cdot}Cl + H_2O_2 \rightarrow {}^{\cdot}HO_2 + H^+ + Cl^- \qquad \text{(Equation 18)}$$

Figure 4. Effect of initial catholyte pH

(A) H_2O_2 production, (B) current efficiency in the scaled-up MES reactor, and (C) pH variation during the process.
Operating conditions: input voltage of 0.6 V, cathodic aeration velocity of 0.045 mL min^{-1} mL^{-1}, and electrolyte nature and concentration of 50 mM Na_2SO_4, respectively.

$$CO_3^{2-} + H_2O \leftrightarrow HCO_3^- + OH^- \qquad \text{(Equation 19)}$$

$$CO_3^{2-} + {}^{\bullet}OH \rightarrow {}^{\bullet}CO_3^- + OH^- \qquad \text{(Equation 20)}$$

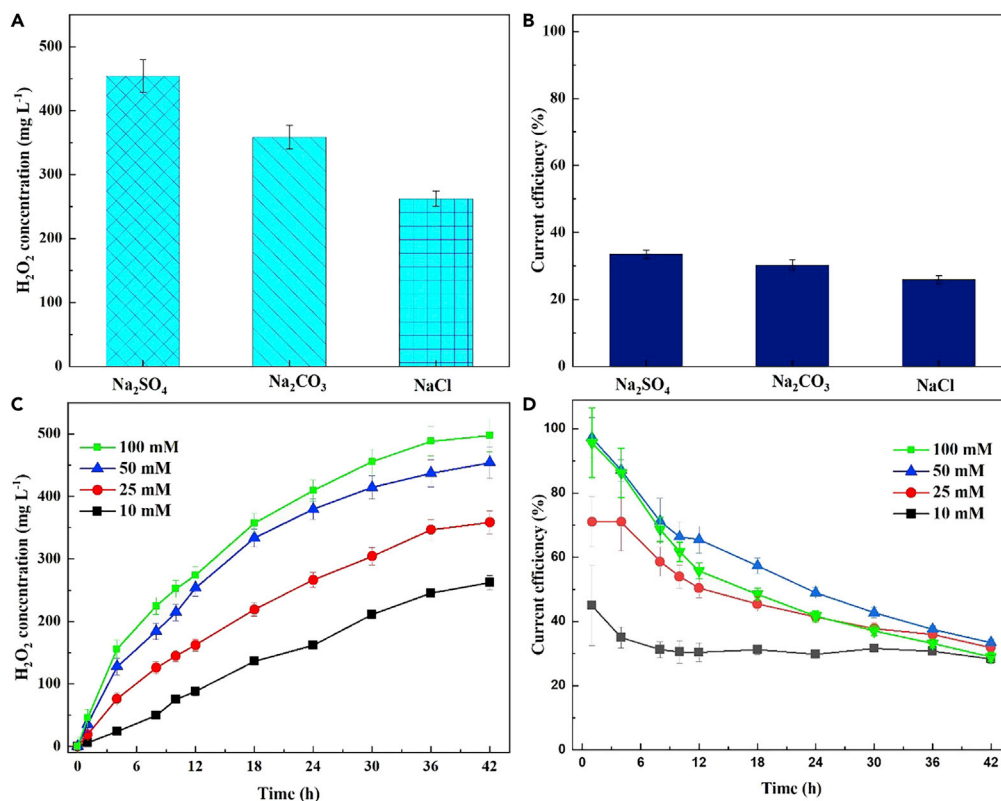$$HCO_3^- + H_2O_2 \rightarrow HCO_4^- + H_2O \qquad \text{(Equation 21)}$$

Figure 5. Effect of electrolyte nature and concentration

(A and C) H_2O_2 production and (B and D) current efficiency in the scaled-up MES reactor. Operating conditions: input voltage of 0.6 V, cathodic aeration velocity of 0.045 mL min^{-1} mL^{-1}, and electrolyte nature (NaCl, Na_2SO_4 and Na_2CO_3), and initial Na_2SO_4 concentration of 10, 25, 50, and 100 mM, respectively.

$$^\bullet CO_3^- + H_2O_2 \rightarrow HCO_3^- + {}^\bullet HO_2 \qquad \text{(Equation 22)}$$

(3) compared with NaCl and Na_2CO_3, Na_2SO_4 has higher conductivity (9.02 ms cm^{-1} vs 8.02 ms cm^{-1} of Na_2CO_3 and 5.66 ms cm^{-1} of NaCl) and correspondingly higher current (see Figure S5) when the initial concentration was 50 mM, and thus, it has the highest production of H_2O_2 (Zhou et al., 2007).

Although the side reactions listed earlier that can affect the synthesis of H_2O_2 will also produce some free radicals with strong oxidizing ability (e.g., $^\bullet Cl$ and $^\bullet OH$), the amount of those strong oxidizing agents produced is very small. Notably, the successful application of bioelectrochemical synthesis of H_2O_2 for the disinfection of gray water and wetland effluent has been recently reported (Arends et al., 2014; Murawski, 2018). However, the dose of H_2O_2 needed to reach the target fecal coliform level in a real municipal effluent from the wastewater treatment plant ranged from 106 to 285 mg L^{-1}, which made the direct application of H_2O_2 as a disinfectant very inappropriate (Wagner et al., 2002). Furthermore, our previous study has also shown that the bioelectrochemical synthesis of H_2O_2 has a poor killing effect on *E. coli* with an initial concentration of 10^7 CFU mL^{-1}, whereas the combination of H_2O_2-producing MEC with Fenton process, named bio-electro-Fenton process, exhibited a significant improvement on the *E. coli* inactivation (Zhou et al., 2018). Besides, a recent study exhibited that the strong alkaline catholyte (pH > 13) produced by the MFC-based electro-osmosis process can effectively inactivate pathogens, but considering its pH also limits its subsequent application to the disinfection of real wastewater (Gajda et al., 2020). In general, although beneficial attempts have been made to directly apply bioelectrochemical systems for water disinfection, considering the treatment efficiency, integration of bioelectrochemical synthesis of H_2O_2 with other advanced oxidation processes (e.g., Fenton process) may be a more promising way for simultaneous

water disinfection and micro-pollutants removal. It was also worth noting that although the application of Na_2CO_3 and NaCl also yielded higher H_2O_2 production, the presence of chloride ions (only when solution pH below 7.2) and carbonates may affect the subsequent application of the synthesized H_2O_2 for wastewater treatment (e.g., they have a scavenging effect on the free radicals [e.g., $^{\bullet}OH$] in Fenton reaction, Chen et al., 2019; Kläning and Wolff, 1985; Zhang et al., 2018). Based on the above, Na_2SO_4 was used as an electrolyte in the subsequent experiments.

Besides the electrolyte nature, the electrolyte concentration, which was related to the conductivity, was also crucial for the electrosynthesis of H_2O_2. Thus, different concentrations of Na_2SO_4 (10, 25, 50, and 100 mM) corresponding to the conductivities of 2.44, 4.95, 9.02, and 16.36 ms cm^{-1}, respectively, were tested. As shown in Figures 5C and 5D, the increase of Na_2SO_4 from 10 to 100 mM increased the continuous improvement of cathodic H_2O_2 accumulation. When the Na_2SO_4 concentration was further increased from 50 to 100 mM, the increase in the H_2O_2 synthesis was getting slower. The correlation between electrolyte concentration and H_2O_2 synthesis can be explained as follows. First, the conductivity was higher with higher electrolyte concentration applied, which further increased the current (see Figure S6), thereby promoting the production of H_2O_2 (Zhou et al., 2007). Second, to a certain extent (e.g., below 200 mM), increasing the Na_2SO_4 concentration could increase the mass transfer, thereby increasing the H_2O_2 synthesis (Jin et al., 2014). Third, excessive Na_2SO_4 may be adsorbed on the surface of the electrode, resulting in a decrease in the active site that can bind to oxygen molecules on the electrode, which in turn reduces to produce H_2O_2 (Chen et al., 2015b). Last, excessive Na_2SO_4 could also consume the generated H_2O_2 via Equations 23 and 24 (Jin et al., 2014).

$$SO_4^{2-} + {}^{\bullet}OH \rightarrow {}^{\bullet}SO_4^- + OH^- \qquad \text{(Equation 23)}$$

$$^{\bullet}SO_4^- + H_2O_2 \rightarrow SO_4^{2-} + H^+ + {}^{\bullet}HO_2 \qquad \text{(Equation 24)}$$
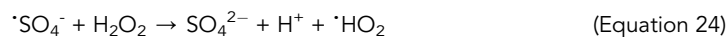
Although the addition of 100 mM Na_2SO_4 resulted in the highest concentration of H_2O_2, it was considered that there was only a small increase compared with that at 50 mM. In addition, considering the cost of chemicals and the subsequent cost of further desalination, 50 mM Na_2SO_4 was selected for the subsequent test.

Energy consumption and performance comparison

To comprehensively understand the feasibility of the scaled-up MES for the *in situ* electrosynthesis of H_2O_2, the energy consumption required for the entire process under the selected optimal conditions was further calculated. The energy consumption calculation can be divided into two aspects, one was from the input voltage required by the reactor itself, and another was from cathodic aeration using a pump. For the first aspect, the calculated energy consumption was 0.298 kWh kg^{-1} H_2O_2 (Supplemental information). More-over, for the second aspect, the energy consumption by the pump within 42 h was recorded as 0.42 kWh, equal to 99.291 kWh kg^{-1} H_2O_2. Therefore, the total energy consumption was 99.587 kWh kg^{-1} H_2O_2, of which approximately 99.70% was consumed by the pump for the cathodic aeration. It was mainly due to extremely low oxygen utilization efficiency (calculated value was 1.43% based on the formula reported in the previous literature) (Yu et al., 2015b). However, low oxygen utilization efficiency was a common phenomenon in which graphite plate was used as electrodes (Yu et al., 2015b). Recently, Zhang et al. reported a superhydrophobic natural air diffusion electrode, which had an oxygen utilization efficiency of up to 65% when used in the synthesis of H_2O_2 (Zhang et al., 2020). This provided a solution for the subsequent application of the scaled-up MES system to efficiently synthesize H_2O_2 and further reduce the energy consumption caused by aeration. In addition, it should be pointed out that the energy consumption for H_2O_2 synthesis based on electrochemical systems or bioelectrochemical systems reported in the literature almost did not take into account the energy consumption including pumping for aeration, and most of the aeration rates adopted in the literature were similar to or slightly higher than that adopted in this study.

Additionally, Table 1 compared the energy consumption of this scaled-up MES with previously published studies. First, although the traditional electrochemical systems (e.g., electro-Fenton) in the laboratory scale using graphite as the cathode have slightly higher H_2O_2 production rate compared with the scaled-up MES in this study, the energy consumption was much higher in the traditional electrochemical systems. Second, compared with laboratory-scale MFC systems that did not require additional voltage input, the scaled-up

Table 1. Previous studies on H_2O_2 production through (bio)electrochemical systems

System Types	Cathode Materials	Operating Conditions	Reactor Volume	H_2O_2 Production Rate	Energy Consumption	References
Electro-Fenton	Graphite	pH of 2, 50 mM NaClO$_4$, cathodic aeration rate of 8,747 mL min^{-1}, and applied cathode potential of -0.5 versus SCE	7.65 L (3.15 L of cathode)	40.6 mg L^{-1} h^{-1}	7.8 kWh kg^{-1} H_2O_2	(Qiang et al., 2002)
MEC	Vulcan carbon-coated GDE	pH of 7, 200 mM NaCl, cathodic aeration rate of 20 mL min^{-1}, and applied voltage of 0.31 V	218 mL (18 mL of cathode)	8.8 mg L^{-1} h^{-1}	1.1 kWh kg^{-1} H_2O_2	(Young et al., 2016)
MEC	GDE	pH of 7, 50 mM NaCl, and applied voltage of 0.9 V	18.8 mL (9.4 mL of cathode)	4.2 mg L^{-1} h^{-1}	1.8 kWh kg^{-1} H_2O_2	(Modin and Fukushi, 2012)
MEC	Electrochemically modified graphite particle	pH of 7, 50 mM NA$_2$SO$_4$, and applied voltage of 0.4 V	96 mL (64 mL of cathode)	88.2 mg L^{-1} h^{-1}	0.66 kWh kg^{-1} H_2O_2	(Chen et al., 2015a, 2015b)
MEC	Carbon black and graphite hybrid air cathode	pH of 7, 50 mM NaCl, cathodic aeration rate of 1,500 mL min^{-1}, and applied voltage of 0.6 V	42 mL (14 mL of cathode)	3.3 mg L^{-1} h^{-1}	56 kWh kg^{-1} H_2O_2	(Li et al., 2016)
MEC	Carbon GDE	Tap water, cathodic aeration rate of 2,000 mL min^{-1}, and applied voltage of 1.0–1.6 V (CEM) or 1.6–2.0 V(AEM)	110 L (10 L of cathode)	0.019 mg L^{-1} h^{-1} (AEM) and 0.274 mg L^{-1} h^{-1} (CEM)	–	(Sim et al., 2018)
MFC	3D graphite cathode	pH of 7 and 50 mM NA$_2$SO$_4$	82 mL (50 mL of cathode)	1.5 mg L^{-1} h^{-1}	–	(Li et al., 2018a, 2018b)
MFC	Graphite	pH of 7 and 100 mM Na$_2$SO$_4$ and cathodic aeration rate of 191 mL min^{-1}	160 mL (80 mL of cathode)	6.6 mg L^{-1} h^{-1}	–	(Fu et al., 2010)
MFC	Electrochemically modified graphite/ carbon black/active carbon particle	pH of 7 and 50 mM NA$_2$SO$_4$	204.5 mL (120 mL of cathode)	6.8/7.1/8.1 mg L^{-1} h^{-1}	–	(Chen et al., 2014)
MREC	Graphite	pH of 7, 35 g L^{-1} NaCl, cathodic aeration rate of 12 mL min^{-1}, and salt and fresh water flow rate of 0.5 mL min^{-1}	140 mL (40 mL of cathode)	10.80 mg L^{-1} h^{-1}	0.45 kWh kg^{-1} H_2O_2	(Li et al., 2017)
20-L scaled-up MES reactor	Graphite	pH of 3, 50 mM NA$_2$SO$_4$, cathodic aeration rate of 400 mL min^{-1}, and applied voltage of 0.6 V	20 L (10 L of cathode)	10.82 mg L^{-1} h^{-1}	0.298 kWh kg^{-1} H_2O_2	In this study

AEM, anion exchange membrane; MREC, microbial reverse-electrodialysis electrolysis cell

MES exhibited a faster H_2O_2 production rate with little energy consumption (0.298 kWh kg^{-1} H_2O_2). Last, compared with the laboratory-scale MEC systems, the scaled-up MES exhibited not only lower energy consumption but also faster H_2O_2 production rate. Besides, Table 1 also showed that the H_2O_2 production rate (88.20 vs 10.82 mg L^{-1}) of some MEC systems was higher than that of this study because modified GDE was used in these studies. The reason can be attributed to the fact that the pumped oxygen can be absorbed by the porous structure of the GDE instead of being dissolved in the catholyte, which overcomes the limitation of low H_2O_2 production usually caused by low oxygen solubility (Yu et al., 2015b). However, using GDE may increase the capital cost in the practical application and may cause water leakage when applied to the

scaled-up systems (Wang et al., 2020a). There was only one literature in the form of short communication that reported an MEC system with equivalent cathodic volume as in this study, but the reported H_2O_2 production rate was much lower and the energy consumption was expected to be higher because of the higher aeration rate and input voltage adopted. Finally, it should be pointed out that the cathode potential measured during the whole experiment is higher than $-0.86V$, which indicated that the corrosion of the graphite electrode can be effectively avoided in this scaled-up system, thereby achieving a long lifespan (Qiao et al., 2018).

Limitation of the study

Although promising, there are still several bottlenecks that need to be further addressed. First, in this study, the electrolyte (e.g., 50 mM Na_2SO_4) was added to increase the system current and therefore the production of H_2O_2, which would lead to an increase in operating cost. Future large-scale applications should be concentrated on high-conductivity wastewater (e.g., textile wastewater) or combined with a membrane technology to treat concentrates (e.g., reverse osmosis). Moreover, the cathodic oxygen utilization rate was low, which was manifested as the cathodic aeration provided by the pump occupying around 99.70% of the total energy consumption. This challenge could be solved in the future through optimization of the reactor configuration and the development of new electrode materials with higher oxygen mass transfer efficiency.

Resource availability

Lead contact

Further information and requests for resources and materials should be directed to and will be fulfilled by the Lead Contact, Yifeng Zhang (yifz@env.dtu.dk, yifzmfc@gmail.com).

Materials availability

This study did not yield new unique reagents.

Data and code availability

There is no dataset or code associated with this work.

METHODS

All methods can be found in the accompanying Transparent Methods supplemental file.

SUPPLEMENTAL INFORMATION

Supplemental Information can be found online at https://doi.org/10.1016/j.isci.2021.102094.

AUTHOR CONTRIBUTIONS

R.Z.: Methodology, validation, formal analysis, writing – original draft. A.H.: Methodology, validation, formal analysis. A.K.: Resources, supervision, validation. X.Y.: Investigation, visualization. M.X.: Investigation, visualization. I.A.: Resources, supervision, validation, funding acquisition. Y.Z.: Conceptualization, resources, supervision, funding acquisition.

DECLARATION OF INTERESTS

The authors declare no competing interests.

REFERENCES

An, J., Li, N., Zhao, Q., Qiao, Y., Wang, S., Liao, C., Zhou, L., Li, T., Wang, X., and Feng, Y. (2019). Highly efficient electro-generation of H_2O_2 by adjusting liquid-gas-solid three phase interfaces of porous carbonaceous cathode during oxygen reduction reaction. Water Res. *164*, 114933.

Arends, J.B., Van Denhouwe, S., Verstraete, W., Boon, N., and Rabaey, K. (2014). Enhanced disinfection of wastewater by combining wetland treatment with bioelectrochemical H_2O_2 production. Bioresour. Technol. *155*, 352–358.

Attiogbe, F.K., and Francis, R.C. (2011). Hydrogen peroxide decomposition in bicarbonate solution catalyzed by ferric citrate. Can. J. Chem. *89*, 1289–1296.

Brillas, E., Maestro, A., Moratalla, M., and Casado, J. (1997). Electrochemical extraction of oxygen from air via hydroperoxide ion. J. Appl. Electrochem. *27*, 83–92.

Campos-Martin, J.M., Blanco-Brieva, G., and Fierro, J.L. (2006). Hydrogen peroxide synthesis: an outlook beyond the anthraquinone process. Angew. Chem. Int. Ed. *45*, 6962–6984.

Chen, F., Xia, L., Zhang, Y., Bai, J., Wang, J., Li, J., Rahim, M., Xu, Q., Zhu, X., and Zhou, B. (2019). Efficient degradation of refractory organics for carbonate-containing wastewater via generation carbonate radical based on a photoelectrocatalytic TNA-MCF system. Appl. Catal. B Environ. *259*, 118071.

Chen, J.-y., Li, N., and Zhao, L. (2014). Three-dimensional electrode microbial fuel cell for hydrogen peroxide synthesis coupled to wastewater treatment. J. Power Sources *254*, 316–322.

Chen, J.-y., Zhao, L., Li, N., and Liu, H. (2015a). A microbial fuel cell with the three-dimensional electrode applied an external voltage for synthesis of hydrogen peroxide from organic matter. J. Power Sources *287*, 291–296.

Chen, J., Xia, Y., and Dai, Q. (2015b). Electrochemical degradation of chloramphenicol with a novel Al doped PbO_2 electrode: performance, kinetics and degradation mechanism. Electrochim. Acta *165*, 277–287.

Chen, S., Chen, Z., Siahrostami, S., Kim, T.R., Nordlund, D., Sokaras, D., Nowak, S., To, J.W., Higgins, D., and Sinclair, R. (2018). Defective carbon-based materials for the electrochemical synthesis of hydrogen peroxide. ACS Sustain. Chem. Eng. *6*, 311–317.

Chung, T.H., Meshref, M.N., Hai, F.I., Al-Mamun, A., and Dhar, B.R. (2020). Microbial electrochemical systems for hydrogen peroxide synthesis: Critical review of process optimization, prospective environmental applications, and challenges. Bioresour. Technol. 123727.

De Laat, J., Le, G.T., and Legube, B. (2004). A comparative study of the effects of chloride, sulfate and nitrate ions on the rates of decomposition of H_2O_2 and organic compounds by Fe (II)/H_2O_2 and Fe (III)/H_2O_2. Chemosphere *55*, 715–723.

Fabian, I. (1995). Mechanistic aspects of ozone decomposition in aqueous solution. Prog. Nucl. Energy *29*, 167–174.

Freakley, S.J., Piccinini, M., Edwards, J.K., Ntainjua, E.N., Moulijn, J.A., and Hutchings, G.J. (2013). Effect of reaction conditions on the direct synthesis of hydrogen peroxide with a AuPd/TiO_2 catalyst in a flow reactor. ACS Catal. *3*, 487–501.

Fu, L., You, S.J., Yang, F.l., Gao, M.m., Fang, X.h., and Zhang, G.q. (2010). Synthesis of hydrogen peroxide in microbial fuel cell. J. Chem. Technol. Biotechnol. *85*, 715–719.

Gajda, I., Obata, O., Greenman, J., and Ieropoulos, I.A. (2020). Electroosmotically generated disinfectant from urine as a by-product of electricity in microbial fuel cell for the inactivation of pathogenic species. Sci. Rep. *10*, 1–10.

Hassan, M., Olvera-Vargas, H., Zhu, X., Zhang, B., and He, Y. (2019). Microbial electro-Fenton: an emerging and energy-efficient platform for environmental remediation. J. Power Sources *424*, 220–244.

Jin, P., Chang, R., Liu, D., Zhao, K., Zhang, L., and Ouyang, Y. (2014). Phenol degradation in an electrochemical system with TiO_2/activated carbon fiber as electrode. J. Environ. Chem. Eng. *2*, 1040–1047.

Kelly, S.R., Shi, X., Back, S., Vallez, L., Park, S.Y., Siahrostami, S., Zheng, X., and Nørskov, J.K. (2019). ZnO as an active and selective catalyst for electrochemical water oxidation to hydrogen peroxide. ACS Catal. *9*, 4593–4599.

Kläning, U.K., and Wolff, T. (1985). Laser flash photolysis of HClO, ClO^-, HBrO, and BrO^- in aqueous solution. Reactions of Cl-and Br-atoms. Berichte Bunsenges. für Phys. Chem. *89*, 243–245.

Lai, X., Ning, X.-a., Chen, J., Li, Y., Zhang, Y., and Yuan, Y. (2020). Comparison of the Fe^{2+}/H_2O_2 and Fe^{2+}/PMS systems in simulated sludge: removal of PAHs, migration of elements and formation of chlorination by-products. J. Hazard. Mater. 122826.

Li, N., An, J., Zhou, L., Li, T., Li, J., Feng, C., and Wang, X. (2016). A novel carbon black graphite hybrid air-cathode for efficient hydrogen peroxide production in bioelectrochemical systems. J. Power Sources *306*, 495–502.

Li, N., Wang, S., An, J., and Feng, Y. (2018a). Acid pretreatment of three-dimensional graphite cathodes enhances the hydrogen peroxide synthesis in bioelectrochemical systems. Sci. Total Environ. *630*, 308–313.

Li, X., Angelidaki, I., and Zhang, Y. (2017). Salinity-gradient energy driven microbial electrosynthesis of hydrogen peroxide. J. Power Sources *341*, 357–365.

Li, X., Chen, S., Angelidaki, I., and Zhang, Y. (2018b). Bio-electro-Fenton processes for wastewater treatment: advances and prospects. Chem. Eng. J. *354*, 492–506.

Logan, B.E., and Regan, J.M. (2006). Electricity-producing bacterial communities in microbial fuel cells. Trends Microbiol. *14*, 512–518.

Luo, H., Li, C., Wu, C., and Dong, X. (2015a). In situ electrosynthesis of hydrogen peroxide with an improved gas diffusion cathode by rolling carbon black and PTFE. Rsc Adv. *5*, 65227–65235.

Luo, H., Li, C., Wu, C., Zheng, W., and Dong, X. (2015b). Electrochemical degradation of phenol by in situ electro-generated and electro-activated hydrogen peroxide using an improved gas diffusion cathode. Electrochim. Acta *186*, 486–493.

Modin, O., and Fukushi, K. (2012). Development and testing of bioelectrochemical reactors converting wastewater organics into hydrogen peroxide. Water Sci. Technol. *66*, 831–836.

Moreira, F.C., Boaventura, R.A., Brillas, E., and Vilar, V.J. (2017). Electrochemical advanced oxidation processes: a review on their application to synthetic and real wastewaters. Appl. Catal. B Environ. *202*, 217–261.

Murawski, E.L. (2018). Optimizing Cathode Catalyst Loading in Microbial Peroxide-Producing Cells for Greywater Disinfection. https://tigerprints.clemson.edu/all_theses/2923.

Nadais, H., Li, X., Alves, N., Couras, C., Andersen, H.R., Angelidaki, I., and Zhang, Y. (2018). Bio-electro-Fenton process for the degradation of non-steroidal anti-inflammatory drugs in wastewater. Chem. Eng. J. *338*, 401–410.

Nidheesh, P., and Gandhimathi, R. (2012). Trends in electro-Fenton process for water and wastewater treatment: an overview. Desalination *299*, 1–15.

Oturan, M.A., Sirés, I., and Zhou, M. (2018). Electro-Fenton Process: New Trends and Scale-Up (Springer Singapore).

Perry, S.C., Pangotra, D., Vieira, L., Csepei, L.-I., Sieber, V., Wang, L., de León, C.P., and Walsh, F.C. (2019). Electrochemical synthesis of hydrogen peroxide from water and oxygen. Nat. Rev. Chem. *3*, 442–458.

Qiang, Z., Chang, J.-H., and Huang, C.-P. (2002). Electrochemical generation of hydrogen peroxide from dissolved oxygen in acidic solutions. Water Res. *36*, 85–94.

Qiao, M.-X., Zhang, Y., Zhai, L.-F., and Sun, M. (2018). Corrosion of graphite electrode in electrochemical advanced oxidation processes: degradation protocol and environmental implication. Chem. Eng. J. *344*, 410–418.

Salmerón, I., Plakas, K.V., Sirés, I., Oller, I., Maldonado, M.I., Karabelas, A.J., and Malato, S. (2019). Optimization of electrocatalytic H_2O_2 production at pilot plant scale for solar-assisted water treatment. Appl. Catal. B Environ. *242*, 327–336.

Sheng, H., Janes, A.N., Ross, R.D., Kaiman, D., Huang, J., Song, B., Schmidt, J., and Jin, S. (2020). Stable and selective electrosynthesis of hydrogen peroxide and the electro-fenton process on $CoSe_2$ polymorph catalysts. Energy Environ. Sci. *13*, 4189–4203.

Sheng, Y., Song, S., Wang, X., Song, L., Wang, C., Sun, H., and Niu, X. (2011). Electrogeneration of hydrogen peroxide on a novel highly effective

acetylene black-PTFE cathode with PTFE film. Electrochim. Acta *56*, 8651–8656.

Siahrostami, S., Verdaguer-Casadevall, A., Karamad, M., Deiana, D., Malacrida, P., Wickman, B., Escudero-Escribano, M., Paoli, E.A., Frydendal, R., and Hansen, T.W. (2013). Enabling direct H_2O_2 production through rational electrocatalyst design. Nat. Mater. *12*, 1137–1143.

Sim, J., Reid, R., Hussain, A., An, J., and Lee, H.-S. (2018). Hydrogen peroxide production in a pilot-scale microbial electrolysis cell. Biotechnol. Rep. *19*, e00276.

Wagner, M., Brumelis, D., and Gehr, R. (2002). Disinfection of wastewater by hydrogen peroxide or peracetic acid: development of procedures for measurement of residual disinfectant and application to a physicochemically treated municipal effluent. Water Environ. Res. *74*, 33–50.

Wang, J., Li, C., Rauf, M., Luo, H., Sun, X., and Jiang, Y. (2020a). Gas diffusion electrodes for H_2O_2 production and their applications for electrochemical degradation of organic pollutants in water: a review. Sci. Total Environ. *759*, 143459.

Wang, W., Lu, X., Su, P., Li, Y., Cai, J., Zhang, Q., Zhou, M., and Arotiba, O. (2020b). Enhancement of hydrogen peroxide production by electrochemical reduction of oxygen on carbon

nanotubes modified with fluorine. Chemosphere *259*, 127423.

Xia, G., Lu, Y., and Xu, H. (2015). An energy-saving production of hydrogen peroxide via oxygen reduction for electro-Fenton using electrochemically modified polyacrylonitrile-based carbon fiber brush cathode. Sep. Purif. Technol. *156*, 553–560.

Xia, L., Chen, F., Li, J., Chen, S., Bai, J., Zhou, T., Li, L., Xu, Q., and Zhou, B. (2020). Efficient organic pollutants conversion and electricity generation for carbonate-containing wastewater based on carbonate radical reactions initiated by $BiVO_4$-Au/PVC system. J. Hazard. Mater. *389*, 122140.

Young, M.N., Links, M.J., Popat, S.C., Rittmann, B.E., and Torres, C.I. (2016). Tailoring microbial electrochemical cells for production of hydrogen peroxide at high concentrations and efficiencies. ChemSusChem *9*, 3345–3352.

Yu, F., Wang, Y., Ma, H., and Dong, G. (2018). Enhancing the yield of hydrogen peroxide and phenol degradation via a synergistic effect of photoelectrocatalysis using a g-C_3N_4/ACF electrode. Int. J. Hydrog. Energy *43*, 19500–19509.

Yu, F., Zhou, M., and Yu, X. (2015a). Cost-effective electro-Fenton using modified graphite felt that dramatically enhanced on H_2O_2 electro-generation without external aeration. Electrochim. Acta *163*, 182–189.

Yu, X., Zhou, M., Ren, G., and Ma, L. (2015b). A novel dual gas diffusion electrodes system for efficient hydrogen peroxide generation used in electro-Fenton. Chem. Eng. J. *263*, 92–100.

Zhang, W., Zhou, S., Sun, J., Meng, X., Luo, J., Zhou, D., and Crittenden, J. (2018). Impact of chloride ions on UV/H_2O_2 and UV/persulfate advanced oxidation processes. Environ. Sci. Technol. *52*, 7380–7389.

Zhao, Q., An, J., Wang, X., and Li, N. (2020). In-situ hydrogen peroxide synthesis with environmental applications in bioelectrochemical systems: a state-of-the-art review. Int. J. Hydrog. Energy *46*, 3204–3219.

Zhang, Q., Zhou, M., Ren, G., Li, Y., Li, Y., and Du, X. (2020). Highly efficient electrosynthesis of hydrogen peroxide on a superhydrophobic three-phase interface by natural air diffusion. Nat. Commun. *11*, 1–11.

Zhou, M., Yu, Q., Lei, L., and Barton, G. (2007). Electro-Fenton method for the removal of methyl red in an efficient electrochemical system. Sep. Purif. Technol. *57*, 380–387.

Zhou, S., Huang, S., Li, X., Angelidaki, I., and Zhang, Y. (2018). Microbial electrolytic disinfection process for highly efficient Escherichia coli inactivation. Chem. Eng. J. *342*, 220–227.

Supplemental information

Scaling-up of microbial electrosynthesis

with multiple electrodes for *in situ*

production of hydrogen peroxide

Rusen Zou, Aliyeh Hasanzadeh, Alireza Khataee, Xiaoyong Yang, Mingyi Xu, Irini Angelidaki, and Yifeng Zhang

Supplemental Information

Scaling-up of microbial electrosynthesis with multiple electrodes for in-situ production of hydrogen peroxide

Rusen Zou[1], Aliyeh Hasanzadeh[2], Alireza Khataee[3,4], Xiaoyong Yang[1], Mingyi Xu[1], Irini Angelidaki[1] and Yifeng Zhang[1,5]*

[1] Department of Environmental Engineering, Technical University of Denmark, DK-2800 Lyngby, Denmark

[2] Process and Systems Engineering Center (PROSYS), Department of Chemical and Biochemical Engineering, Technical University of Denmark, Kgs. Lyngby, Denmark

[3] Research Laboratory of Advanced Water and Wastewater Treatment Processes, Department of Applied Chemistry, Faculty of Chemistry, University of Tabriz, 51666-16471, Tabriz, Iran

[4] Peoples' Friendship University of Russia (RUDN University), 6 Miklukho-Maklaya Street, Moscow, 117198, Russian Federation

[5] Lead contact

*Corresponding author:

Dr. Yifeng Zhang

Department of Environmental Engineering, Technical University of Denmark, Denmark

Tel: (+45) 45251410

Fax: (+45) 45933850

E-mail address: yifz@env.dtu.dk; yifzmfc@gmail.com
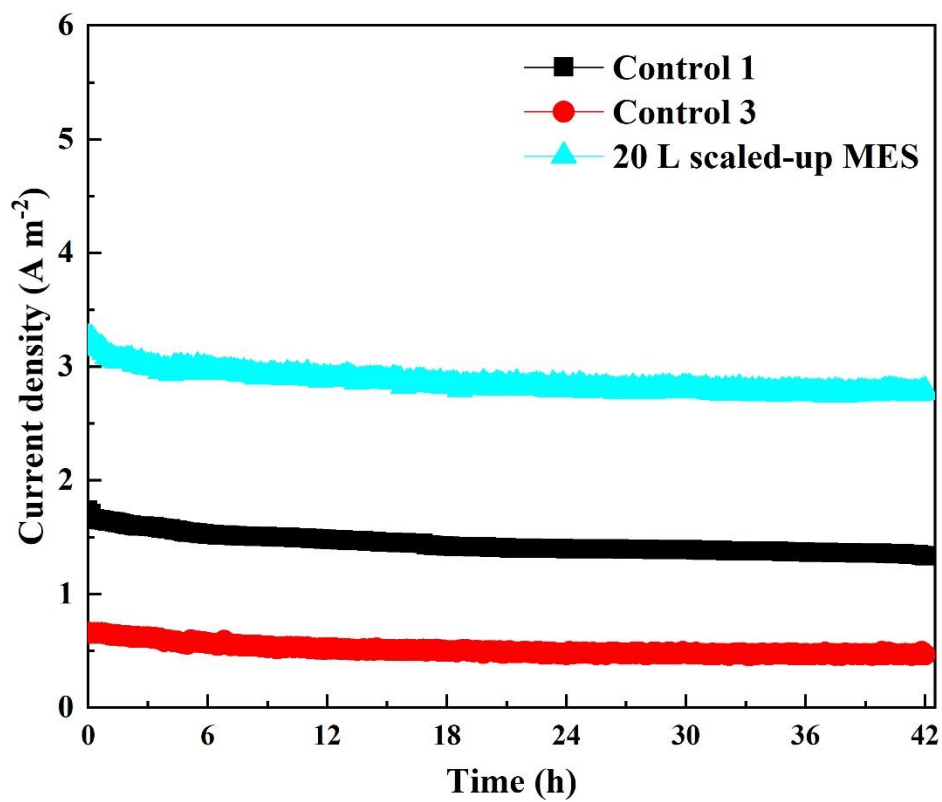
Supplemental Figures

Figure S1. Feasibility verification (current density) of this 20 L scaled-up MES reactor regarding H_2O_2 production, Related to Figure 1.
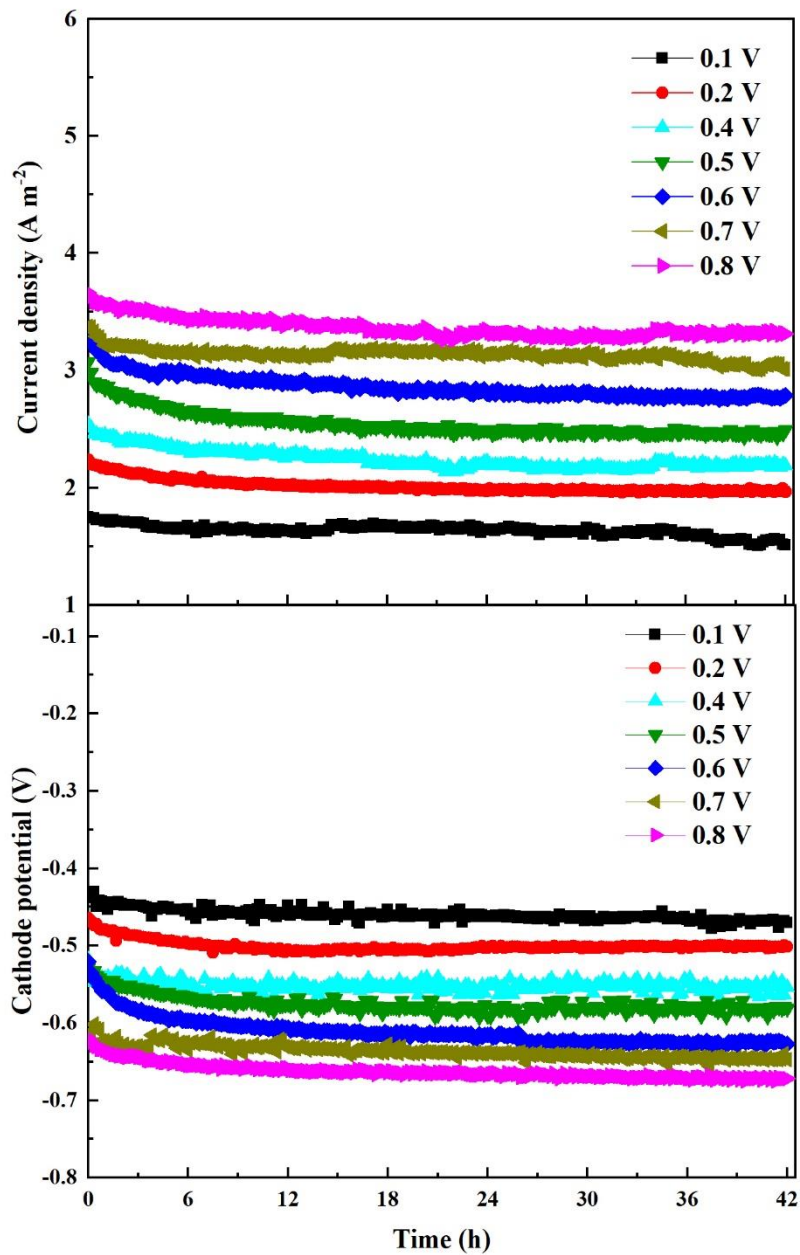
Figure S2. The effect of input voltage (current density and cathode potential) on H₂O₂ production in the scaled-up MES reactor, Related to Figure 2.
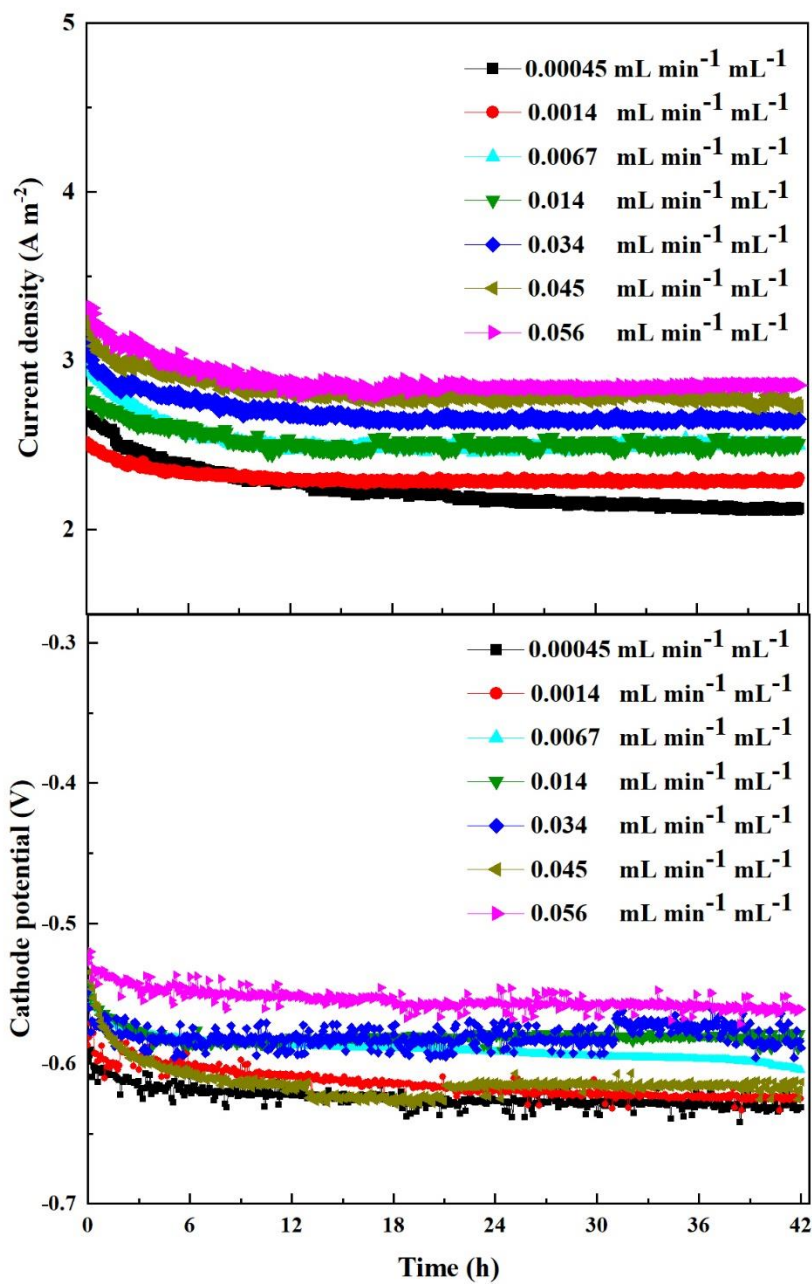
Figure S3. The effect of cathodic areation velocities (current density and cathode potential) on H₂O₂ production in the scaled-up MES reactor, Related to Figure 3.
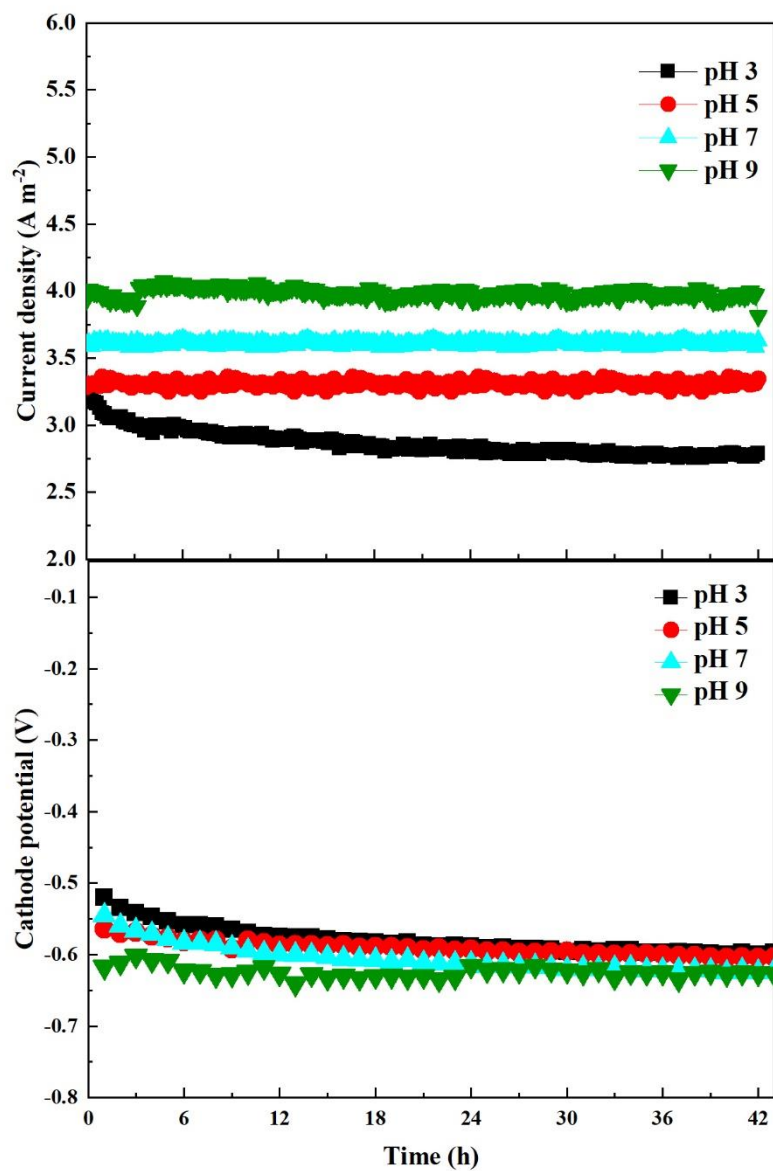
Figure S4. The effect of initial catholyte pH (current density and cathode potential) on H₂O₂ production in the scaled-up MES reactor, Related to Figure 4.
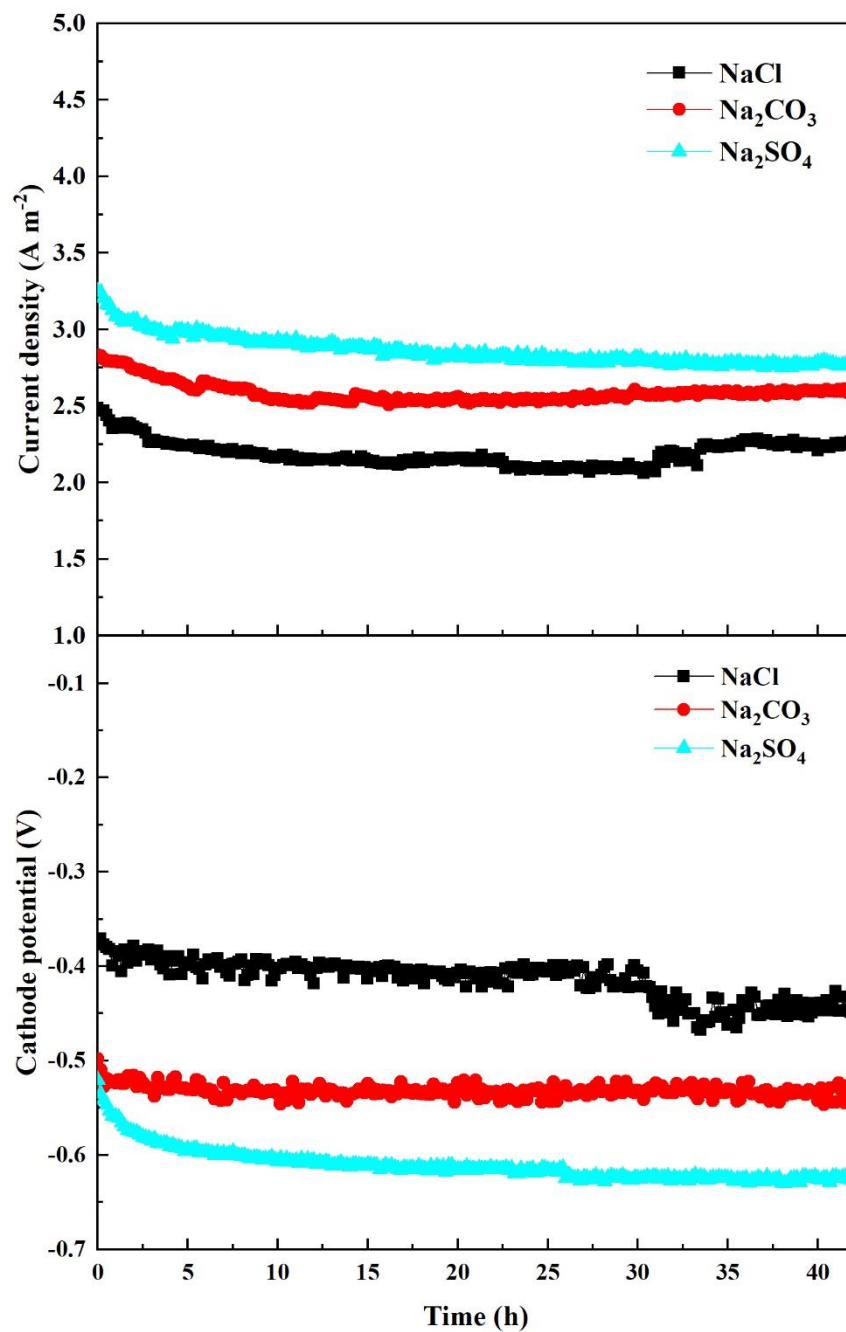
Figure S5. The effect of electrolyte nature (current density and cathode potential) on H₂O₂ production in the scaled-up MES reactor, Related to Figure 5 (a) and (b).
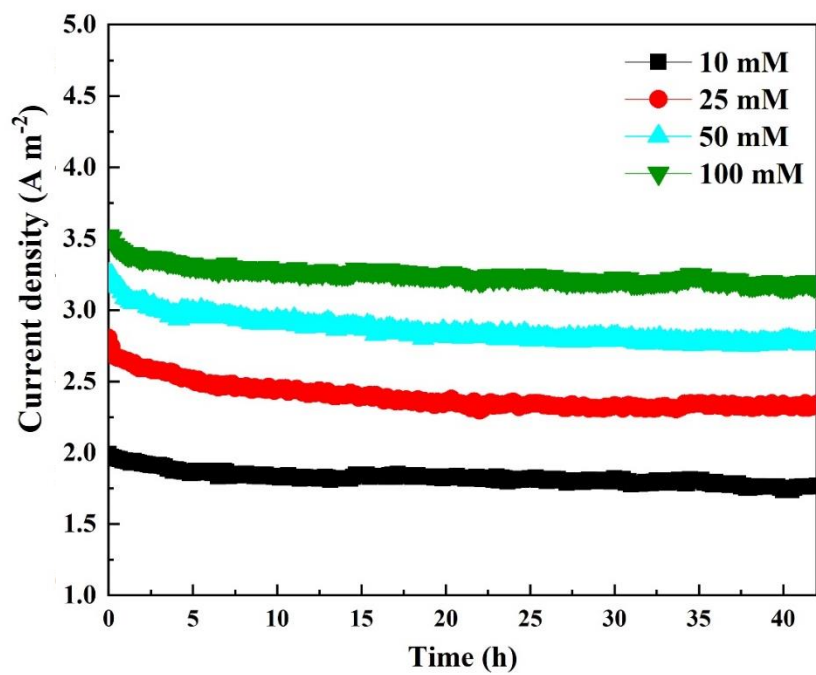
Figure S6. The effect of electrolyte nature concentration (current density) on H₂O₂ production in the scaled-up MES reactor, Related to Figure 5 (c) and (d).
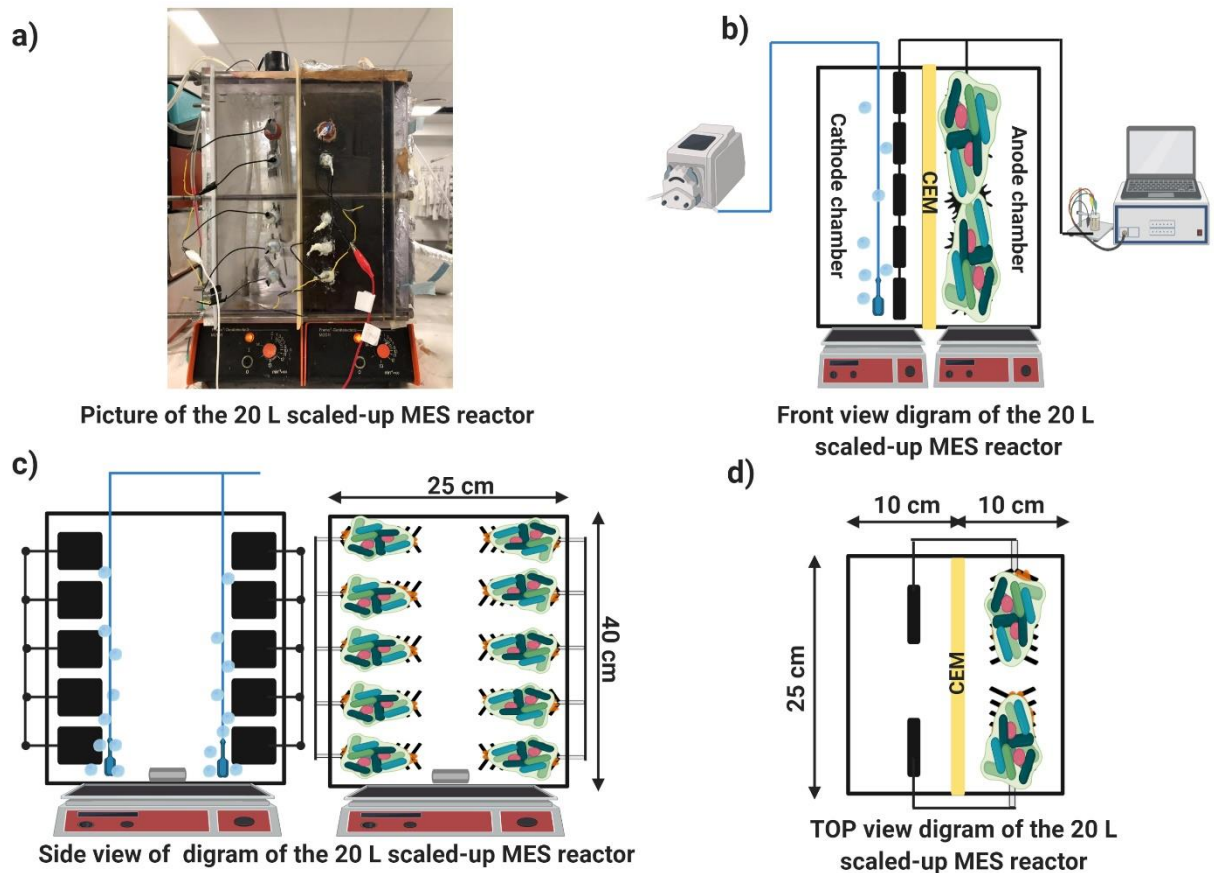
a) Picture of the 20 L scaled-up MES reactor

b) Front view digram of the 20 L scaled-up MES reactor

Cathode chamber CEM Anode chamber

c) Side view of digram of the 20 L scaled-up MES reactor

25 cm

40 cm

d) TOP view digram of the 20 L scaled-up MES reactor

10 cm 10 cm

25 cm

CEM

Fig.S7. Picture and schematic diagram of the 20 L scaled-up MES reactor, Related to Figure 1 and Transparent Methods. (a) Picture of 20 L scaled-up MES reactor. (b) Front view diagram of 20 L scaled-up MES reactor. (c) Side view diagram of 20 L scaled-up MES reactor. (d) Top view diagram of 20 L scaled-up MES reactor.

Transparent Methods

Chemicals

Sodium carbonate (Na_2CO_3, ≥ 99%), sodium chloride (NaCl, ≥ 99.5%), methanol (≥ 99.9%), sodium sulfate (Na_2SO_4, ≥ 99%), sulfuric acid (H_2SO_4, 95-98%), sodium thiosulfate ($Na_2S_2O_3$, ≥ 98%), potassium titanium oxide oxalate dihydrate ($C_4K_2O_9Ti \cdot 2H_2O$) H_2O_2 solution (30 wt. %), and sodium hydroxide (NaOH, ≥ 99%) were purchased from Sigma Aldrich (Denmark).

Reactor configuration and operation

In this study, we designed and assembled a scaled-up MES reactor made of polycarbonate with a total volume of 20 L. The reactor has a two-compartment configuration, separated by a cation exchange membrane (CEM, CMI 7001, Membrane International, NJ), to ensure that protons, one of the metabolites produced at the anode, can be transferred to the cathode and to avoid interference of cathode aeration to the anodic anaerobic environment. The dimensions of the two chambers were identical and the dimensions of a single chamber were specifically 40 cm in length, 10 cm in width, and 20 cm in height. Each corresponding chamber was equipped with 10 electrodes, of which carbon brushes (diameter 5.9 cm, length 6.9 cm, Mill-Rose, USA) were used for the anode electrode and graphite plates were used for the cathode electrode (length 4.5 cm, width 4.5 cm), respectively. Among them, the carbon brushes and CEM were pre-treated before installation and the specific pre-treatment methods can be found in our previous studies (Li et al., 2017; Zhang et al., 2015). In addition, an Ag/AgCl reference electrode (+0.197 V vs SHE, Pine Instrument Company, USA) was installed in the cathode chamber to monitor the cathode potential. Besides, the cathode chamber was also equipped with two microporous aerators with an aeration aperture

of 5 to 100 µm for supplying oxygen to the electrodes immersed in the electrolyte. The specific installation positions of the above-mentioned electrodes and aerators were presented in Fig. S7. When the reactor was assembled, it entered the enrichment phase, which aimed to form mature electrochemical active biofilms on the anode. At this phase, the reactor was operated in MFC mode, with a 1000 ohm resistor connected in series between the anode and cathode. It should be noted that the anodic inoculation was taken from the influent of the wastewater treatment plant (Lundtofte, Copenhagen, Denmark) and amended with 1 g L^{-1} sodium acetate. For the cathode electrolyte, a 50 mM potassium ferricyanide solution containing a 50 mM phosphate buffer (pH at 7) was used. After a one-month enrichment, the reactor can output a stable and repeatable voltage (up to 0.7 V). After that, the reactor was switched to MEC mode operation, and the applied voltage was set to 0.3 V. During this period, the series resistance between the two poles was reduced from 1000 ohms to 0.1 ohms. Notably, synthetic medium was used as the anolyte to avoid the influence of possible changes in real wastewater properties and substrate limitations on anode performance. The anolyte was continuously fed through a 4-channel peristaltic pump (104 RA-CH.4, OLE DICH, Denmark) and hydraulic retention time (HRT) was set for 58 h. Here, the peristaltic pump also provided the function of aeration for the cathode to further lower the overall energy consumption. The specific ingredient of the anodic synthetic medium was the same as previously described (Zhou et al., 2018). In addition, the catholyte was changed from potassium ferricyanide solution to Na_2SO_4 solution, that was, 50 millimoles of Na_2SO_4 was dissolved in 1L of deionized water. Finally, the influence of various operating parameters including input voltage, cathodic aeration velocity, catholyte pH, and electrolyte nature and concentration on the performance of the scaled-up MES for the synthesis of H_2O_2 were studied.

Analytical methods and calculations

The pH values of all samples were determined by a pH meter (PHM 210, radiometer). The dissolved oxygen (DO) of the catholyte was detected by using a digital DO meter (Multi 3420, WTW, UK) equipped with an optical IDS DO sensor (FDO 925, WTW, UK). The concentration of H_2O_2 was detected by the spectrophotometric method (Spectronic 20D+, Thermo, Scientific) as described previously (Sellers, 1980). A battery tester/cycle instrument (CT-4008W, Neware, China) was used to provide input voltage and monitor system current and cathode potential. The current density (A m^{-2}) obtained in this study was calculated based on Eq. (1).

$$\text{Current density (A m}^{-2}) = \frac{I}{S} \quad (1)$$

where I is the recorded current (A), S is the total cathode surface area (m^2).

In addition, the current efficiency (CE, %) of H_2O_2 produced by the scaled-up MES was calculated according to Eq. (2).

$$CE\ (\%) = \frac{nFVC}{Q} \times 100 \quad (2)$$

where n is the number of electrons transferred per mole H_2O_2 generated (2 mol e$^-$/mol H_2O_2) F is Faraday's number (96,485 C/mol e$^-$), V is the catholyte volume (9 L), C is the concentration of H_2O_2 measured, and Q is the cumulative coulombs during operation (C).

Furthermore, the electrical energy consumption was calculated according to Eq. (3).

$$\text{Energy consumption} = \frac{1000UIt}{CV} + \frac{1000W}{CV} \quad (3)$$

where W (kWh) is the electrical energy consumption for aeration and stirring, which was measured by a spar meter (Type NZR230, S.L. Energitekinik, Denmark), U is the applied voltage (V), I is the current (A), t is the electrolysis time (h), C is the concentrated H_2O_2 (mg L^{-1}), and V is the solution volume (L).

Lastly, all the experiments were conducted in triplicate and run at room temperature (25 ± 5 °C).

Supplemental References

Li, X., Jin, X., Zhao, N., Angelidaki, I. and Zhang, Y. (2017). Novel bio-electro-Fenton technology for azo dye wastewater treatment using microbial reverse-electrodialysis electrolysis cell. Bioresour. Technol., 228, 322-329.

Sellers, R.M. (1980). Spectrophotometric determination of hydrogen peroxide using potassium titanium (IV) oxalate. Analyst 105(1255), 950-954.

Zhang, Y., Wang, Y. and Angelidaki, I. (2015). Alternate switching between microbial fuel cell and microbial electrolysis cell operation as a new method to control H_2O_2 level in Bioelectro-Fenton system. J. Power Sources, 291, 108-116.

Zhou, S., Huang, S., Li, X., Angelidaki, I. and Zhang, Y. (2018). Microbial electrolytic disinfection process for highly efficient Escherichia coli inactivation. Chem. Eng. J., 342, 220-227.